 DOI: 10.21608/adjalexu.2022.128039.1264

EFFECT OF GINKGO BILOBA LOADED CHITOSAN SCAFFOLD ON HEALING OF BONE DEFECTS IN RABBIT

Doha M. El-Sayed[1]* *BDs*, Amel R. El-Hak[2] *PhD*, Dina A. Nagui[3] *PhD*, Hossam El-Din M. Mostafa[4] *PhD*

ABSTRACT

INTRODUCTION: Critical sized bone defects do not heal completely by themselves and require intervention by using bone grafts or scaffolds. Chitosan (CS) is a widely used biomaterial for bone regeneration. Ginkgo biloba (GB) leaf's extract is thought to be effective in stimulating bone cells differentiation. Polylactic-co-glycolic acid (PLGA) nanoparticles are commonly used as drug delivery vehicles. The PLGA nanoparticles were loaded with GB and incorporated in CS sponge scaffold.
OBJECTIVES: To evaluate the effect of GB loaded PLGA nanoparticles incorporated in CS scaffold on healing of critical sized bone defects in rabbit.
MATERIALS AND METHODS: eighteen adult male New Zealand rabbits were randomly divided into 3 equal groups (six rabbits each): Group A (Control group), Group B (CS group) and Group C (GB+PLGA+CS group). Critical sized bone defects were performed in the edentulous area of rabbit mandibles (diastema). Group A: defects were left empty, Group B: defects were filled with unloaded CS scaffold, while in group C: defects were filled with CS scaffold incorporated with GB loaded PLGA nanoparticles. Animals were euthanized four weeks after surgery and the results were evaluated histologically and histomorphometrically.
RESULTS: GB loaded scaffold had a great effect on promoting regeneration of bone within the defects.
CONCLUSION: the GB loaded CS scaffold is effective in bone regeneration and the GB extract has an osteoinductive potential.
KEYWORDS: Ginkgo biloba, PLGA nanoparticles, Chitosan, Bone defect, Bone regeneration
RUNNING TITLE: Effect of GB-loaded CS scaffold on bone regeneration.

1. Assistant Lecturer of Oral Biology -Faculty of Dentistry –Alexandria University
2. Professor of Oral Biology -Faculty of Dentistry –Alexandria University
3. Assistant professor of Oral Biology- Faculty of Dentistry - Alexandria University
4. Lecturer of Oral Biology- Faculty of Dentistry - Alexandria University

* *Corresponding Author:*
E-mail: doha.abaza200@gmail.com

INTRODUCTION

One of the most challenging things in the clinical practice is restoration of critical sized bone defects that may result from injuries, infections, tumors and resection surgeries (1). They can be defined as defects that do not heal spontaneously during the lifetime of the animal, they exhibit restricted bone formation at the peripheral defect margins and may become filled with fibrous tissue (2).
Autografts are considered to be the "gold standard" for repair and reconstruction of large bone defects but they have some limitations as they require a second surgery at the donor site, and they also provide insufficient supply (3).
The limitations of autografts may be overcome by using Allografts and xenografts. However, those alternatives have the possibility of eliciting an immune response and rejection by the body as well as pathogens exposure (4).

As the field of tissue engineering develops, scaffolds are becoming widely used as an alternative to allografts and
autografts owing to exhibiting less antigenicity and lack of secondary traumatic approach (5, 6). Scaffolds used for this
process should mechanically support the regenerating tissue, be able to deliver bioactive agents, and fit well in defect to restore functional anatomy (7).
Scaffolds derived from natural polymers such as collagen, fibrin and chitosan are widely used for bone regeneration. CS is a highly versatile, biocompatible and biodegradable biomaterial (8, 9). CS scaffolds has been widely utilized in bone tissue engineering as they exhibit osteoconductivity in surgically created bone defects allowing the

adhesion and proliferation of bone-forming osteoblast cells (10, 11).

Chitosan can be processed in several ways and fabricated into various forms like films, fibers, membranes and sponges (12). However, studies have shown that CS should be integrated with other biomaterials in order to achieve superior mechanical and biological properties (13).

Integrating bone tissue-engineered scaffolds with osteoinductive factors is very important to enhance their osteogenic potential. Incorporating scaffolds with growth factors especially bone morphogenetic proteins render them osteoinductive. However, growth factors are very expensive and may elicit inflammatory reactions (14).

Ginkgo biloba is one of the oldest species of trees that originates from China and contains flavonoids, terpene, and organic acids in its leaf extract. The standardized extract of GB is known as EGB761, which lacks components that may cause toxicity or allergy, it is widely promoted because of its antioxidant and anti-inflammatory effects (15, 16).

Ginkgo biloba was found to be effective in stimulating the proliferation of osteoblast-like bone cells and protecting them against free-radical damage, it also promotes osteoblast differentiation and anti-osteoclastic activity in vitro (17, 18).

There is a significant difficulty in delivering such compound to the target site and using it locally in bone defects which reduces its effectiveness. To overcome these obstacles, drug delivery systems have been developed to allow delivery of biological agents to the target tissues without influencing the non-targeted sites and without undesirable side effects (19).

Polylactic acid-co-glycolic acid is an FDA approved synthetic polymer that can be used as a carrier or a drug delivery vehicle in a form of nanospheres or microspheres owing to their great biocompatibility, controllable biodegradability, and excellent interaction with biomolecules (20).

Polylactic acid-co-glycolic acid is a combination of the polymers polylactic acid (PLLA) and polyglycolic acid (PGA) and it's one of the most commonly used biodegradable polymers in tissue engineering applications. The higher the ratio of PGA within a PLGA scaffold, the faster the degradation rate. The byproducts of its degradation are less acidic and nontoxic (21).

In the present study, CS scaffold was fabricated in a sponge form and incorporated with GB-loaded PLGA nanoparticles (22). Studies available about using this scaffold in vivo in bone defects regeneration are limited. Thus, the present study aims at clarifying this point by evaluating its biological effect on healing of mandibular critical sized bone defects in rabbits.

The null hypothesis in the present investigation proposes that there will be no significant difference between the newly fabricated GB loaded PLGA/CS scaffold compared to the unloaded CS scaffold and the control group regarding healing of mandibular critical sized bone defects in rabbits

MATERIALS AND METHODS

This study design was approved by the Ethical Committee of Faculty of Dentistry, Alexandria University. The approval number by the ethical committee is 0203 and IORG 0008839.

Experimental animals

18 adult male rabbits were used in this study. Animals were obtained from the animal house of Medical Research Institute, Alexandria University. They were kept under the same environmental conditions in the experimental animal house. Rabbits were randomly assigned by using computer generated random numbers (23) to one of three equal groups (6 rabbits each) (24):

Group A : Negative control, where critical sized bone defects were left empty.

Group B : Positive control, defects were filled with unloaded CS scaffold.

Group C : Study group, defects were filled with GB loaded PLGA nanoparticles incorporated in CS scaffold in a sponge form.

Materials

1- GB fluid extract obtained from Nature's Answer company (NY, United States).
2- CS scaffold and (GB/PLGA/CS) scaffold were prepared and purchased from Nano Gate© company (Nano Gate, Nasr city, Cairo, Egypt).
3- Trephine surgical bur purchased from MCTBIO Co. (South Korea).

Surgical procedure

General anesthesia was induced by an intramuscular injection of a combination of 25mg/kg weight ketamine and 5mg/kg body weight xylazine. The edentulous alveolar ridges of the mandible between the incisor and the first posterior tooth (diastema) on the right side of each rabbit were selected for the surgical site. Full mucoperiosteal flaps were raised and Osseous defects (3 mm length x3mm width x3mm depth) were prepared using a sterile trephine surgical bur under water cooling system to make sure that all the defects would have standardized size and shape. The bone defects performed in each animal were washed out with sterile saline and left empty in group A, filled with CS scaffold in group B while in group C defects were filled with GB/PLGA/CS scaffold. After the surgical procedure, rabbits were monitored for any symptoms and the operative sites were monitored daily. All rabbits were given broad-spectrum antibiotics in a form of intramuscular injection and diclofenac sodium IM analgesic every eight hours for the first two days following surgery (25).

Euthanasia

Rabbits were euthanized after four weeks (N=18 rabbits) by intravenous injection with a lethal dose (100 mg/kg) of pentobarbital sodium. The rabbits were decapitated, and the mandibles were dissected

out. In each group, mandibular specimens were prepared for histological evaluation by light microscope and histomorphometric analysis (26).

Scanning electron microscopy (SEM) Characterization of the scaffold

The morphology of the unloaded CS and the fabricated (GB/PLGA/CS) scaffold was examined with scanning electron microscopy (Faculty of Science, Alexandria University). The scaffolds were cut by a razor blade and mounted on aluminum stubs with conductive paint and then sputter-coated with gold for examination (22). The structural morphology of CS scaffold as well as GB/PLGA/CS scaffold showed a porous microstructure including macro and micro pores that appear to be interconnected and randomly oriented.

(Figure 1 and 2)

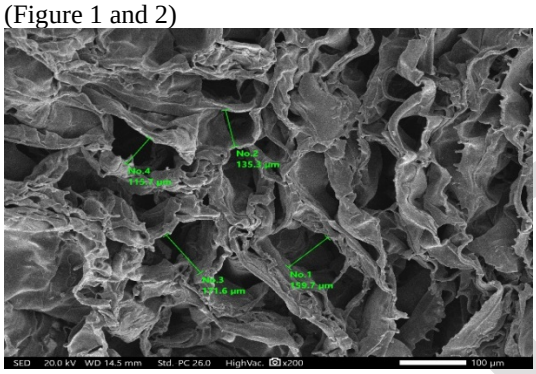

Figure 1: SEM of CS scaffold showing highly porous structure with randomly oriented and interconnected pores (x200).

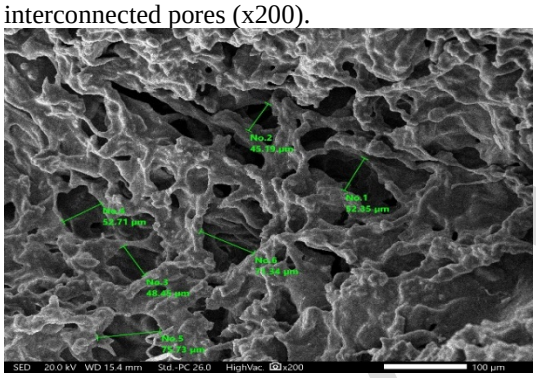

Figure 2: SEM of GB/PLGA/CS scaffold showing highly porous trabecular like structure with randomly oriented and interconnected pores (x200).

Characterization of the PLGA nanoparticles

The size and shape of GB-loaded PLGA nanoparticles were determined using Transmission Electron Microscope (TEM) (Faculty of Science, Alexandria University) (22). The TEM image showed spherical particles with regular outline and a smooth surface. Average particle size ranging from 100-125 nanometer. (Figure 3)

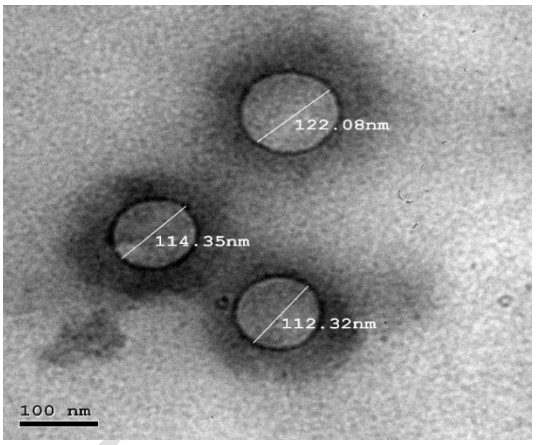

Figure 3: TEM of PLGA nanoparticles suspension showing that the nanoparticles are spherical and regular in shape with average particle size ranging from 100-125 nm. Scale bar 100 nm.

Histological examination

Specimens were fixed in 10 % neutral-buffered formalin, washed, decalcified with 8% trichloroacetic acid, dehydrated with ascending concentrations of ethanol, cleared with xylene, and embedded in paraffin wax blocks. Mesio-distal sections of the mandibular defects were cut at a 4 µm thickness and stained with Hematoxylin and Eosin (H&E). Sections were examined by light microscope for histological evaluation of bone healing (27).

Histomorphometric measument

Computer assisted histomorphometry was performed in H&E sections in order to measure the percentage of newly formed bone surface area compared to the total surface area of the osseous defect after 4 weeks in pixels of 40x magnification in the different groups by using image J software analyze system (28).

Statistical analysis

Data of the histomorphometric measurements were analyzed using IBM SPSS software package version 24.0. Comparison between the three groups was done by using F-test (ANOVA) followed by post hoc test to compare between each two groups. Data were expressed as mean and standard deviation; significance of the results was judged at the 5% level.

RESULTS

1. Histological results

Group A: Control group

The control group images showed newly formed woven bone along the peripheral areas of the defect with large number and size of osteocytes as well as irregular course of collagen fibers. The central part of the defect appeared empty with no bone formation. A line of demarcation denoting fusion between the newly formed bone and the native bone. (Figure 4A and 4B)

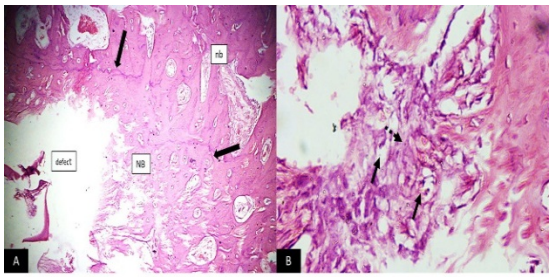

Figure 4: LM (control group), **A:** showing; newly formed bone in the peripheral areas of the bone defect. Note the line of demarcation (arrows) between newly formed bone (NB) and native bone (nb). (H&E stain X 40). **B:** showing; newly formed woven bone in the bone defect. Note the presence of large number and size of osteocytes (black arrows) and the irregular course of collagen fibers of the newly formed bone (dashed arrow). (H&E stain X400).

Group B: CS group

The CS scaffold was partially replaced by fibrous tissue and newly formed bone at the peripheral parts of the defect. The walls of the defect were lined by voluminous active osteoblasts and numerous osteocytes, while the central part of the defect was occupied by the CS scaffold. (Figure 5A and 5B)

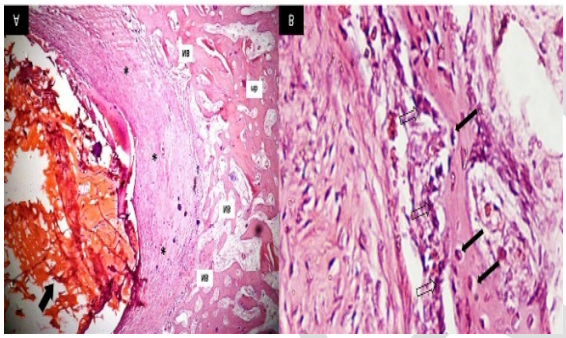

Figure 5: LM (CS scaffold group). **A:** showing; the chitosan scaffold (black arrow) occupying the central part of the defect and it is partially replaced by fibrous tissue (asterisks) and newly formed bone (NB). nb=native bone. (H&E stain X40). **B:** showing, the newly formed bone lined by voluminous osteoblasts (hollow arrows) and contains numerous osteocytes (black arrows). (H&E stain X400).

Group C: GB/PLGA/CS group

The scaffold was partially replaced and surrounded by abundant amount of newly formed bone with primary osteons and several reversal lines. Voluminous osteoblasts were also noted. The central part of the defect was filled with the GB/PLGA/CS scaffold which has a trabecular like structure. More amount of bone and less fibrous tissue are surrounded the scaffold compared to group B. (Figure 6A and 6B)

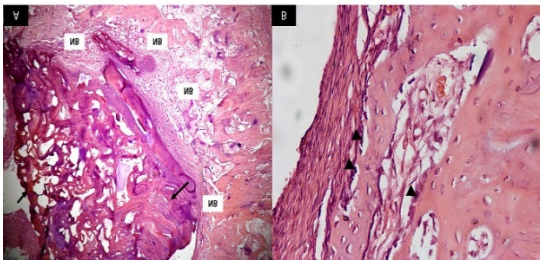

Figure 6: LM (GB/PLGA/CS scaffold group), **A:** showing; the material (black arrow) is partially replaced and surrounded by abundant amount of newly formed bone (NB). (H&E stain X40). **B:** showing, newly formed bone with numerous primary osteons and reversal lines. Note the presence of voluminous osteoblast cells (arrow heads). (H&E stain X400).

2. Histomorphometric and statistical analysis

The percentage of the bone surface area formed within the defect was measured in the three groups which was demonstrated in Table (1). All groups showed new bone formation within the defect. The percentage of bone was higher in both the CS group and the GB/PLGA/CS group compared to the control group and the difference was statistically significant for the GB/PLGA/CS group ($P<0.001$) and not significant for the CS group ($P<0.09$). More bone was formed in the GB/PLGA/CS group compared to the empty CS group. However, the difference was statistically insignificant ($P<0.18$). (Table 1)

Table (1): The percentage of the bone surface area formed within the defects in the three groups.

	Control group	**CS scaffold**	**GB/PLGA/CS scaffold**
Mean	37.05	48.41	58.86
S.D.	4.42	16.24	13.64
ANOVA P value	0.002*		
P1 P2 P3		0.09	0.001* 0.18

P was significant if ≤ 0.05

P1 comparison between control group and CS scaffold

P2 comparison between control group and GB-PLGA-CS scaffold group

P3 comparison between CS scaffold and GB-PLGA-CS scaffold group

DISCUSSION

The ideal scaffold for bone tissue engineering should not only serve as a matrix for cell adhesion and proliferation, it should also contain osteoinductive factors that induce the differentiation of bone forming cells (14). The CS scaffold was incorporated with GB-loaded PLGA nanoparticles to allow the delivery of GB to promote the osteogenic potential of the scaffold. The present study showed that using the GB loaded CS scaffold is an effective approach for

bone regeneration. The great regenerative capacity of the scaffold was evaluated and confirmed in vivo by promoting bone regeneration within a 3x3x3-mm rabbit mandibular bone defect.

Ginkgo biloba leaf's extract is widely used for the treatment of various bone related diseases (29). However, systemic administration of GB is limited by low drug availability and relatively short half-life (30). In order to enhance drug bioavailability and avoid undesirable effects, GB was encapsulated into PLGA nanoparticles that allows sustainable and controlled release of GB extract at the target site of action (31).

The obtained nanoparticles were regular and spherical in shape with smooth surface which was in agreement with previous studies done by Ezirganlı S et al. and Li Y et al. (2, 31).

The osteogenic potential of the GB-loaded CS scaffold was assessed using critical-sized bone defects in rabbit mandibles, since it is a reliable technique to evaluate the effect of such material on bone regeneration (26). Four weeks following the surgical procedure, the histological sections showed evident bone regeneration and active bone formation in both unloaded and GB loaded CS scaffold groups with more abundant bone formation and less fibrous tissue encapsulation in the GB/PLGA/CS scaffold group. These results coincide with the results of previous studies performed by Oh SM et al. and Lucinda et al. which indicated respectively that GB extract stimulated the in vitro differentiation of osteoblast cells and inhibited their apoptosis by increasing the expression of the anti-apoptotic protein called Bcl-2 protein (18, 32). GB extract was also found to promote healing of bone fractures, possess an anti-osteoporotic activity, and it inhibits osteoclastic bone resorption (29, 33).

Quantitative results yielded from histomorphometrical analysis showed the positive effect of GB loaded scaffold on bone regeneration with the highest percentage of newly formed bone within the defect compared to the control group and the unloaded chitosan group and this may be attributed to the synergistic effect of the CS and the GB extract released from the nanoparticles. And these results come in agreement with Sun et al. who indicated that the osteogenic potential of the scaffolds should be enhanced by combining them with osteoinductive agents (34).

The histological sections also indicated the presence of the scaffolds inside the bone defects as they are only partially degraded at this point, and they require more time to be fully degraded after implantation in vivo. Chitosan scaffolds require few months to fully degrade depending on the processing and deacetylation from chitin polymer. Higher deacetylation would lead to slower degradation and vice versa (35). However, the scaffold should not degrade too fast in order to perform its action and it's not meant to stay in the defect for a very long time as it hinders healing and regeneration (36).

CONCLUSION

This study verifies that the CS scaffold incorporated with GB loaded PLGA nanoparticles is effective in bone regeneration owing to the osteoinductive potential of GB extract. Thus, this triad maybe promising for treating critical-sized bone defects.

CONFLICT OF INTEREST

Authors declare having no conflicts of interests.

FUNDING

No specific funding was received for this work.

REFERENCES

1. Agarwal R, García AJ. Biomaterial strategies for engineering implants for enhanced osseointegration and bone repair. Adv Drug Deliv Rev. 2015;94:53-62.
2. Ezirganlı Ş, Kazancıoğlu HO, Mihmanlı A, Aydın M, Sharifov R, Alkan A. The effect of local simvastatin application on critical size defects in the diabetic rats. Clin Oral Implants Res. 2014;25:969-76.
3. Ning L, Malmström H, Ren YF. Porous collagen-hydroxyapatite scaffolds with mesenchymal stem cells for bone regeneration. J Oral Implantol. 2015;41:45-9.
4. David F, Levingstone TJ, Schneeweiss W, de Swarte M, Jahns H, Gleeson JP, et al. Enhanced bone healing using collagen-hydroxyapatite scaffold implantation in the treatment of a large multiloculated mandibular aneurysmal bone cyst in a thoroughbred filly. J Tissue Eng Regen Med. 2015;9:1193-9.
5. Pan Z, Ding J. Poly (lactide-co-glycolide) porous scaffolds for tissue engineering and regenerative medicine. Interface Focus. 2012;2:366-77.
6. Park SH, Park DS, Shin JW, Kang YG, Kim HK, Yoon TR, et al. Scaffolds for bone tissue engineering fabricated from two different materials by the rapid prototyping technique: PCL versus PLGA. J Mater Sci Mater Med. 2012;23:2671-8.
7. Hollister SJ, Lin CY, Saito E, Lin CY, Schek RD, Taboas JM, et al. Engineering craniofacial scaffolds. Orthod Craniofac Res. 2005;8:162-73.
8. Lee KY, Jeong L, Kang YO, Lee SJ, Park WH. Electrospinning of polysaccharides for regenerative medicine. Adv Drug Deliv Rev. 2009;61:1020-32.
9. Madihally SV, Matthew HW. Porous chitosan scaffolds for tissue engineering. Biomaterials. 1999;20:1133-42.
10. Horn MM, Martins VC, Plepis AM. Influence of collagen addition on the thermal and morphological properties of chitosan/xanthan hydrogels. Int J Biol Macromol. 2015;80:225-30.
11. Seol YJ, Lee JY, Park YJ, Lee YM, Young K, Rhyu IC, et al. Chitosan sponges as tissue engineering scaffolds for bone formation. Biotechnol Lett. 2004;26:1037-41.

12. Levengood SL, Zhang M. Chitosan-based scaffolds for bone tissue engineering. J Mater Chem B. 2014;2:3161-84.
13. Correia CR, Moreira-Teixeira LS, Moroni L, Reis RL, van Blitterswijk CA, Karperien M, et al. Chitosan scaffolds containing hyaluronic acid for cartilage tissue engineering. Tissue Eng Part C Methods. 2011;17:717-30.
14. Gentile P, Nandagiri VK, Daly J, Chiono V, Mattu C, Tonda-Turo C, et al. Localised controlled release of simvastatin from porous chitosan-gelatin scaffolds engrafted with simvastatin loaded PLGA-microparticles for bone tissue engineering application. Mater Sci Eng C Mater Biol. Appl 2016;59:249-57.
15. Chan PC, Xia Q, Fu PP. Ginkgo biloba leave extract: biological, medicinal, and toxicological effects. J Environ Sci Health C Environ Carcinog Ecotoxicol Rev. 2007;25:211-44.
16. Vilar JB, Leite KR, Chen Chen L. Antimutagenicity protection of Ginkgo biloba extract (Egb 761) against mitomycin C and cyclophosphamide in mouse bone marrow. Genet Mol Res. 2009;8:328-33.
17. Brayboy J, Chen X, Lee Y, Anderson J. The protective effects of Ginkgo biloba extract (EGb 761) against free radical damage to osteoblast-like bone cells (MC3T3-E1) and the proliferative effects of EGb 761 on these cells. Nutr Res. 2001;21:1275-85.
18. Oh SM, Kim HR, Chung KH. Effects of ginkgo biloba on in vitro osteoblast cells and ovariectomized rat osteoclast cells. Arch Pharm Res. 2008;31:216-24.
19. Wilczewska AZ, Niemirowicz K, Markiewicz KH, Car H. Nanoparticles as drug delivery systems. Pharmacol Rep. 2012;64:1020-37.
20. Ghorbani F, Zamanian A, Nojehdehian H. Effects of pore orientation on in-vitro properties of retinoic acid-loaded PLGA/gelatin scaffolds for artificial peripheral nerve application. Mater Sci Eng C Mater Biol Appl. 2017;77:159-72.
21. Lee Y, Kwon J, Khang G, Lee D. Reduction of inflammatory responses and enhancement of extracellular matrix formation by vanillin-incorporated poly (lactic-co-glycolic acid) scaffolds. Tissue Eng Part A. 2012;18:1967-78.
22. Marouf N, Nojehdehian H, Ghorbani F. Physicochemical properties of chitosan–hydroxyapatite matrix incorporated with Ginkgo biloba-loaded PLGA microspheres for tissue engineering applications. Polym Polym Compos. 2020;28:320-30.
23. Suresh K. An overview of randomization techniques: An unbiased assessment of outcome in clinical research. J Hum Reprod Sci. 2011;4:8-11.
24. Song J, Kim J, Woo HM, Yoon B, Park H, Park C, et al. Repair of rabbit radial bone defects using bone morphogenetic protein-2 combined with 3D porous silk fibroin/β-tricalcium phosphate hybrid scaffolds. J Biomster Sci Polym Ed. 2018;29:716-29.
25. Eleftheriadis E, Leventis MD, Tosios KI, Faratzis G, Titsinidis S, Eleftheriadi I, et al. Osteogenic activity of β-tricalcium phosphate in a hydroxyl sulphate matrix and demineralized bone matrix: a histological study in rabbit mandible. J Oral Sci. 2010;52:377-84.
26. Ye P, Yu B, Deng J, She RF, Huang WL. Application of silk fibroin/chitosan/nano-hydroxyapatite composite scaffold in the repair of rabbit radial bone defect. Exp Ther Med. 2017;14:5547-53.
27. Gartner LP. BRS cell biology and histology. Philadelphia: Wolters Kluwer; 2019.
28. Dempster DW, Compston JE, Drezner MK, Glorieux FH, Kanis JA, Malluche H, et al. Standardized nomenclature, symbols, and units for bone histomorphometry: a 2012 update of the report of the ASBMR Histomorphometry Nomenclature Committee. J Bone Miner Res. 2013;28:2-17.
29. Li Z, Li J, Zhao W, Li Y. Potential antiosteoporotic effect of ginkgo biloba extract via regulation of SIRT1-NF-kB signaling pathway. J King Saud Univ Sci. 2020;32:2513-9.
30. Diamond BJ, Shiflett SC, Feiwel N, Matheis RJ, Noskin O, Richards JA, et al. Ginkgo biloba extract: mechanisms and clinical indications. Arch Phys Med Rehabil. 2000;81:668-78.
31. Li Y, Zhang Z, Zhang Z. Porous Chitosan/Nano-Hydroxyapatite Composite Scaffolds Incorporating Simvastatin-Loaded PLGA Microspheres for Bone Repair. Cells Tissues Organs. 2018;205:20-31.
32. Lucinda LMF, Aarestrup BJV, Brandão JS, Peters VM, Reis JE, Guerra MDO. The effect of Ginkgo biloba extract treatment in the Bcl-2 expression by osteoblasts in the femoral trabecular bone of Wistar rats with glucocorticoid-induced osteoporosis. Rev Bras Farmacogn. 2014;24:363-6.
33. Guzel N, Sayit E, Aynaci O, Kerimoglu S, Yulug E, Topbas M. Ginkgo Biloba improves bone formation during fracture healing: an experimental study in rats. Acta Ortop Bras. 2017;25:95-8.
34. Sun H, Wang J, Deng F, Liu Y, Zhuang X, Xu J, et al. Co‐delivery and controlled release of stromal cell‐derived factor‐1α chemically conjugated on collagen scaffolds enhances bone morphogenetic protein‐2‐driven osteogenesis in rats. Mol Med Rep. 2016;14:737-45.
35. Islam N, Dmour I, Taha MO. Degradability of chitosan micro/nanoparticles for pulmonary drug delivery. Heliyon. 2019;5:e01684.
36. Jayasuriya AC, Bhat A. Fabrication and characterization of novel hybrid organic/inorganic microparticles to apply in bone regeneration. J Biomed Mater Res A. 2010;93:1280-8.